



## A Study on State Estimation of Synchronous Generator using an Improved Unscented Kalman Filter Algorithm



Yahaya Ismail<sup>1\*</sup>, Boyi Jimoh<sup>2</sup> and Adamu Saidu Abubakar<sup>3</sup>

<sup>1</sup>Agricultural and Bio-Environmental Technology, Division of Agricultural Collages, Ahmadu Bello University, Zaria-Nigeria.

<sup>2</sup>Department of Electrical Engineering, Ahmadu Bello University, Zaria-Nigeria.

<sup>3</sup>Department of Electrical Engineering, Ahmadu Bello University, Zaria-Nigeria.

\*Corresponding author email: yahayaismail46@gmail.com

### Keywords: –

Improved UKF Algorithm, Nonlinear Filtering, Power Systems, State Estimation, Synchronous Generators,

### Article History: –

Received: 24 Mar, 2025.

Reviewed: 13 May, 2025

Accepted: 23 Oct, 2025

Published: 12 Dec, 2025

### ABSTRACT

*An enhanced Unscented Kalman Filter (UKF) technique for synchronous generator state estimation is presented in this study. The suggested approach overcomes the drawbacks of conventional UKF in managing noise and nonlinearities in power systems. Comparative analysis and validation are made on the tracking performance of Normal Ukf and Improved Ukf (SR-Ukf) algorithms and the simulation results show that, under the same conditions. The Normal UKF produced an RMSE of 0.5390, while the SR UKF achieved a markedly lower RMSE of 0.1540. corresponding to a 71.4% reduction in estimation error. According to simulation results, the enhanced UKF estimates generator states under a range of operating scenarios with more accuracy and robustness.*

## 1. INTRODUCTION

Synchronous generators are the cornerstone of modern power networks, serving as the primary electrical energy source in both conventional and renewable energy-based grids. These devices use the electromagnetic induction principle to convert mechanical energy into electrical energy, providing a reliable and consistent power source to meet the always increasing demand for electricity [1].

Because they produce steady and dependable electrical energy, synchronous generators are essential to power systems. For system stability, control strategy optimization, and catastrophic failure prevention, precise assessment of their dynamic states such as rotor angle, speed, and internal voltages is essential. Nevertheless, the dynamics of synchronous generators are nonlinear, and state estimation is severely hampered by noise and system uncertainties [2].

Due to their dependence on linear approximations, traditional estimate methods like the Extended Kalman Filter (EKF), which have been widely employed, frequently have trouble with highly nonlinear systems. Using a deterministic sampling technique, the Unscented Kalman Filter (UKF) has become a potent substitute that provides better performance by directly capturing the nonlinearities. Notwithstanding its benefits, the conventional UKF has drawbacks that may reduce its usefulness in practical power system applications, such as computational inefficiency and noise sensitivity [3].

This study suggests an enhanced UKF method designed specifically for synchronous generator state estimation. The suggested approach adds improvements like adaptive noise adjustment and optimal sigma point selection to solve the drawbacks of the conventional UKF. Higher estimation accuracy, resilience, and computational efficiency under various operating situations are the goals of these

enhancements. The enhanced UKF's performance is assessed and contrasted with conventional techniques through simulation tests, indicating its potential for real-world power system applications [4].

State estimation for synchronous generators involves determining internal states (e.g., rotor angle, speed, and internal voltages) from available measurements (e.g., terminal voltages, currents, and power). Accurate estimation is crucial for real-time monitoring, control, and stability analysis. Traditional methods like the Extended Kalman Filter (EKF) linearize the nonlinear model, which can lead to inaccuracies. The Unscented Kalman Filter (UKF) addresses this by using a deterministic sampling approach to better capture nonlinearities, making it more suitable for synchronous generator state estimation [5].

This paper is organized as follows: A description of the enhancement of the UKF algorithm is provided in section 2, the mathematical model based on differential Algebraic Equations (DAE) of the type 2-1 model is discussed in section 3. Section 4 presents the simulation results. Finally, conclusions are presented in section 5.

## **2. DYNAMIC STATE ESTIMATION**

State estimation is the process of reconstructing unmeasured internal variables of a system from available measurements. In power systems, state estimation enables operators to monitor hidden generator states such as rotor angle, rotor speed, and internal voltages, which are critical for stability and control but are not directly measurable. Conventional state estimation in power systems is often based on weighted least squares (WLS) methods. While effective for steady-state analysis, WLS techniques are inadequate for capturing nonlinear and time-varying dynamics of generator. This limitation has led to the adoption of dynamic state estimation (DSE) techniques, which rely on

recursive filtering algorithms such as the Kalman Filter.

An SPKF that makes advantage of the unscented transformation is the Ukf, with the help of this transformation, one may determine the statistics of a random variable that has undergone nonlinear mapping [6]. The idea is that "approximating a probability distribution is easier than approximating an arbitrary nonlinear function." A collection of points selected deterministically and a Gaussian random variable (GRV) serve as representations of the state distribution. In addition to reliably capturing the posterior mean and covariance to the third order for Gaussian inputs and the second order for any nonlinearity, these points also record the genuine mean and covariance of the GRV [4].

Since nonlinear systems are involved, many methods, like EKF and UKF, have been developed to estimate the nonlinearities of the system's dynamics [7]. These techniques' shortcomings are examined and criticized. In order to address the filtering problem in nonlinear dynamic systems with random parameters, the improved Ukf (Sqrt-UKF) concepts are put forth in this section. First, the Improved Unscented Transformation was introduced, which uses a nonlinear function with random parameters to propagate the mean and covariance of a random vector [9].

### **2.1 Normal Unscented Kalman filter (UKF) algorithm**

The UKF was implemented as a nonlinear estimation algorithm based on the Unscented Transform (UT). Instead of linearizing the system model as in the Extended Kalman Filter (EKF), the UKF propagates a set of deterministically chosen sigma points through the nonlinear process model. This approach captures the mean and covariance of the system states with higher accuracy [4].

### **2.2 Enhancement of an Unscented Kalman filter (UKF) algorithm**

The SR-UKF is a numerically stable variant of the UKF, in which the square root of the covariance matrix is propagated instead of the full covariance. This

approach reduces computational errors and ensures positive definiteness of the covariance matrix. The SR-UKF follows the same prediction and correction structure as the UKF but performs all covariance updates using Cholesky factorization. This results in improved numerical stability and reduced sensitivity to noise, especially in high-dimensional nonlinear systems such as synchronous generators. Implementing the Square Root Unscented Kalman Filter (UKF) model using MATLAB involves implementing the UKF algorithm and potentially enhancing it with improvements:

The power system can be modeled using the following set of differential and algebraic equations

$$\dot{x} = g(x, \theta, u, w) \quad (1)$$

$$y = l(x, \theta, u, v) \quad (2)$$

where:  $x \in R^n$  is the state variable vector,  $\theta \in R^q$  is the Parameter vector,  $w \in R^n$  is the process noise vector,  $v \in R^m$  is the measurement noise vector,  $g$  and  $l$  are nonlinear differentiable function,  $y \in R^m$  is the measurable vector and  $u \in R^p$  is the input vector [6]. The discretization of the model (2) and (3) is presented as follows:

$$x_k = f(x_{k-1}, \theta_{k-1}, u_{k-1}, w_{k-1}) \quad (3)$$

$$y_k = h(x_k, \theta_k, u_k, v_k) \quad (4)$$

### 2.1.1 Prediction steps

The following procedures are usually used in initializing the state vector, state estimation error covariance matrix and weighted mean and covariance, using the following equations [4]:

$$\hat{X}_0^+ = \in [X_0] \quad (5)$$

$$S_0 = chol(\in (X_0 - \hat{X}_0)(X_0 - \hat{X}_0)^T) \quad (6)$$

$$w^{(m)}_0 = \frac{\lambda}{L + \lambda} \quad (7)$$

$$w^{(c)}_0 = \frac{\lambda}{L + \lambda} + 1 - \alpha^2 + \beta \quad (8)$$

$$w^{(m)}_i = w^{(c)}_i = \frac{1}{2(L + \lambda)} \quad (9)$$

$$i = 1, \dots, 2L$$

where:  $\lambda = L(\alpha^2 - 1)$ ,  $\eta = \sqrt{(L + \lambda)}$ ,  $\beta = 2$

$$\alpha = 1 * 10^{-4} < \alpha < 1$$

In order to capture the entire probabilistic distribution of a random variable, these filters choose a collection of points and then propagates them through the functions  $F(\cdot)$  and  $H(\cdot)$ , which are not limited to being linear. A set of sigma points can be created using the Unscented Transform method using the statistical data (mean and covariance) of the states that are expressed in the equations [7] :

$$X_{k-1} = [\hat{X}_{k-1} \quad \hat{X}_{k-1} \pm \eta S_k] \quad (10)$$

$$X_{k|k-1} = F[X_{k-1}, U_{k-1}] \quad (11)$$

$$\hat{X}_k = \sum_{i=0}^{2L} w_i^{(m)}, X_{i,k|k-1} \quad (12)$$

$$S_k^- = qr\left[\sqrt{W^{(c)}}_i (X_{1:2L,k|k-1} - \hat{X}_k^-) \sqrt{R^v}\right] \quad (13)$$

$$S_k^- = cholupdate(S_k^-, X_{0k} - \hat{X}_k^-, W_0^{(c)}) \quad (14)$$

Procedures generate a set of sigma points that appropriately reflect the uncertainty in the state variables and enable the estimation of the system's state using nonlinear models.

$$y_{k|k-1} = [\hat{y}_{k-1} \quad \hat{y}_{k-1} \pm \eta S_k] \quad (15)$$

$$y_{k|k-1} = H[X_{k|k-1}] \quad (16)$$

Determine the mean and covariance of the model output by using the propagated sigma points and accounting for the nonlinearities in the model. This can be achieved by computing the covariance and weighted averages of the propagated sigma points.

$$\hat{y}_k^- = \sum_{i=0}^{2L} W_i^{(m)}, y_{i,k|k-1} \quad (17)$$

$$S_{y_k}^- = qr\left[\sqrt{W^{(c)}}_i (y_{1:2L,k|k-1} - \hat{y}_k^-) \sqrt{R_k^n}\right] \quad (18)$$

$$S_{y_k}^- = cholupdate(S_{y_k}^-, y_{0k} - \hat{y}_k^-, W_0^{(c)}) \quad (19)$$

### 2.1.2 Measurement Update:

This weighted sum can be used to calculate an estimate of the innovation covariance matrix, which is a representation of the measurement Prediction uncertainty. It offers useful information for further stages of the estimation procedure, such utilizing measurement data to update the state estimate. The innovation covariance matrix as expressed in equations (17) and (18):

By computing this weighted total, one can get an estimate of the cross-covariance matrix, which shows the relationship between the expected state and the projected measurement. It provides valuable information for updating the state estimate using measurement data in later phases of the estimating process and expressed as [4]:

$$P_{x_k y_k} = \sum_{i=0}^{2L} W^{(c)}_i [X_{i,k|k-1} - \hat{X}^-_k] [y_{i,k|k-1} - \hat{y}^-_k]' \quad (20)$$

Calculating the Kalman Gain matrix yields the factor that determines how much the measurement will impact the updated state estimate in the Kalman Filter process. To get the optimum state estimate process, this element is necessary and expressed as:

$$K_k = \frac{\begin{pmatrix} P_{x_k y_k} \\ S^T \hat{y}_k \end{pmatrix}}{S \hat{y}_k} \quad (21)$$

An updated state estimate that incorporates both the measurement data and the expected state, weighted by the Kalman Gain, can be obtained by computing these phases. This updated state provides the best approximation of the system state given the available measurement data, using equation (22) [4].

$$\hat{X}_k = \hat{X}^-_k + K_k (y_k - \hat{y}^-_k) \quad (22)$$

To obtain an updated square root error covariance matrix estimate by using the following equations (23) and (24), by doing the following actions:

$$U = K_k S \hat{y}_k \quad (23)$$

$$S_k = cholupdate(S^-_k, U, -1) \quad (24)$$

Return the augmented state estimation  $\hat{X}_k$ .

where:  $R^v =$  Process noise Covariance,  $R^n =$  Measurement noise Covariance

Also, the weighting vectors  $W^{(m)}$  and  $W^{(c)}$  are calculated using equations (7) to (9) [4].

### 3. Dynamic Model of Synchronous Generator

This section describes the mathematical model based on Differentials Algebraic Equations (DAE) of the sixth order type 2-1 model synchronous generator utilized in this work [8].

#### 3.1 Stator Model of the Synchronous Generator

The stator dynamics were represented in per-unit form, relating the terminal voltages, stator currents, and flux linkages through the following equations:

$$\frac{d\psi_d}{dt} = \omega_b (\omega_r \psi_q + r_a i_d + v_d) \quad (25)$$

$$\frac{d\psi_q}{dt} = \omega_b (-\omega_r \psi_d + r_a i_q + v_q) \quad (26)$$

Where:  $\omega_r \psi_q, \omega_r \psi_d =$  Speed Voltages and

$$\frac{d\psi_d}{dt}, \frac{d\psi_q}{dt} = \text{Transformer Voltages}$$

when analyzing a slow electromechanical transient, the stator transients are disregarded. Transformer voltages are therefore set to zero, and equations 25 and 26 become algebraic equations that can be expressed as follows:

$$0 = \psi_d + v_q + r_a i_q \quad (27)$$

$$0 = -\psi_q + v_d + r_a i_d \quad (28)$$

#### 3.2 Electrical Model of the Synchronous Generator

The rotor dynamics were expressed using differential equations for transient and sub-transient voltages along the q and d -axes:

At d- axis, the differential transient voltage equation can be express as:

$$\frac{de'_d}{dt} = \frac{1}{T'_{d0}} \left( -e'_d + (x_q - x'_q) \left( \frac{(-e'_d + V_h \sin \delta)}{x_q} \right) \right) \quad (29)$$

At d- axis, the differential sub-transient voltage equation can be express as:

$$\frac{de''_d}{dt} = \frac{1}{T''_{d0}} \left( -e''_d + e'_d + (x'_q - x''_q) \left( \frac{(-e'_d + V_h \sin \delta)}{x_q} \right) \right) \quad (30)$$

At q- axis, the differential transient voltage equation can be express as:

$$\frac{de'_q}{dt} = \frac{1}{T'_{d0}} \left( -e'_q - (x_d - x'_d) \left( \frac{(e'_q - V_h \sin \delta)}{x'_d} \right) + E_{fd} \right) \quad (31)$$

At q-axis, the differential sub-transient voltage equation can be express as:

$$\frac{de''_q}{dt} = \frac{1}{T''_{d0}} \left( -e''_q + e'_q - (x'_d - x''_d) \left( \frac{(e'_q - V_h \sin \delta)}{x'_d} \right) \right) \quad (32)$$

### 3.3 Mechanical Model of the Synchronous Generator

Mechanical equations of synchronous generator, the angular position of the rotor with respect to a synchronous rotating reference speed is express as [8]:

$$\frac{d\delta}{dt} = \omega_b (\omega_r - \omega_s) \quad (33)$$

The swing equation of the synchronous generator is expressed as:

$$\frac{d\omega}{dt} = \frac{\omega_b}{2H} \left( T_m - \left( e_d \left( \frac{(-e'_d + V_h \sin \delta)}{x_q} \right) - e_q \left( \frac{(e'_q - V_h \sin \delta)}{x'_d} \right) \right) - D\Delta\omega \right) \quad (34)$$

where  $T_e = P_e = (e_d i_q - e_q i_d)$  is the electromagnetic torque when stator resistance is zero [1].

The algebraic equations are express as:

$$0 = \psi_d + x''_d i_d - e''_q \quad (35)$$

$$0 = \psi_q + x''_q i_q + e''_d \quad (36)$$

### 3.4 Network interface and output of the generator

The single machine infinite bus (SMIB), which converts variables to the synchronous reference frame and saves the line-to-line rms value voltage  $V_h$ , is taken into consideration in order to interface the generator

with the network and carry out system studies. Per-unit is used to express all values. The load can be described as constant impedance, constant power, constant current, or a combination of these. The remaining electric power system is replaced with an infinite bus to make the generator model analysis easier [8]. Using a step-up transformer and a transmission line with equivalent resistance  $R_e$  and impedance  $L_e$ , the generator voltage terminal as stated in (39) is connected to an infinite bus.

$$0 = V_h \sin(\delta) - e_d \quad (37)$$

$$0 = V_h \cos(\delta) - e_q \quad (38)$$

$$\begin{bmatrix} V_0 \\ V_q \\ V_d \end{bmatrix} = V_h \sqrt{3} \begin{bmatrix} 0 \\ -\sin(\delta - \theta) \\ \cos(\delta - \theta) \end{bmatrix} + R_e \begin{bmatrix} i_0 \\ i_q \\ i_d \end{bmatrix} + L_e \begin{bmatrix} i_0 \\ i_q \\ i_d \end{bmatrix} - \omega L_e \begin{bmatrix} i_0 \\ i_q \\ i_d \end{bmatrix} \quad (39)$$

The generator output model at the infinite bus bar are as follows:

$$p_e = \left( V_h \cos(\delta - \theta) + R_a \left( \frac{(-e'_d + V_h \sin \delta)}{x_q} \right) \right) \left( \frac{(-e'_d + V_h \sin \delta)}{x_q} \right) + \left( V_h \sin(\delta - \theta) + R_a \left( \frac{(e'_q - V_h \sin \delta)}{x'_d} \right) \right) \left( \frac{(e'_q - V_h \sin \delta)}{x'_d} \right) \quad (40)$$

$$Q_e = \left( V_h \sin(\delta - \theta) + R_a \left( \frac{(e'_q - V_h \cos \delta)}{x'_d} \right) \right) \left( \frac{(e'_q - V_h \cos \delta)}{x'_d} \right) - \left( V_h \cos(\delta - \theta) + R_a \left( \frac{(-e'_d + V_h \sin \delta)}{x_q} \right) \right) \left( \frac{(-e'_d + V_h \sin \delta)}{x_q} \right) \quad (41)$$

$$V_t = \sqrt{(V_h \cos(\delta - \theta))^2 + (V_h \sin(\delta - \theta))^2} \quad (42)$$

$$I_t = \sqrt{\left( \left( \frac{(e'_q - V_h \cos \delta)}{x'_d} \right)^2 + \left( \frac{(-e'_d + V_h \sin \delta)}{x_q} \right)^2 \right)} \quad (43)$$

$$I_{fd} = \frac{x_d (V_f - e'_d) (x_d - x''_d)}{x''_d} \quad (44)$$

## 4. Simulation Results

A set of variables data array was obtained from the model, described in section 3, using MATLAB and Simulink environment.

Table 1 Initial Values of the Synchronous generator Parameters

| Parameters   | Initial values |
|--|----------------|
| Transient time constant on q-axis ( $T'_{q0}$ )            | 0.23           |
| Sub – transient time constant on the q-axis ( $T''_{q0}$ ) | 0.054          |
| Synchronous reactance on the q-axis ( $x_q$ )              | 0.67           |
| Transient reactance on the q-axis ( $x'_q$ )               | 0.55           |
| Sub – transient reactance on the q-axis ( $x''_{q0}$ )     | 0.19           |
| Transient time constant on d-axis ( $T'_{d0}$ )            | 2.63           |
| Sub – transient time constant on the d-axis ( $T''_{d0}$ ) | 0.066          |
| Synchronous reactance on the d-axis ( $x_d$ )              | 1.09           |
| Transient reactance on the d-axis ( $x'_d$ )               | 0.24           |
| Sub – transient reactance on the d-axis ( $x''_{d0}$ )     | 0.15           |
| Damping coefficient ( $D$ )                                | 2.0            |
| Inertia constant ( $H$ )                                   | 5.06           |
| Mechanical power ( $P_m$ )                                 | 0.8            |

Table 2 shows the estimated internal state variables. The SR-UKF consistently produces estimates closer to the actual measurements than the UKF, for instance, the SR-UKF estimate for  $e'_{q}$ , (-0.1583) is nearly identical to the true value (-0.1584), while the UKF introduces a larger deviation (-0.3784). Similar improvements are observed for the other state variables. This demonstrates that SR UKF is better able to attenuate

measurement noise and maintain accurate state tracking.

Table 2 The Internal state variables of the synchronous generator

| Internal State variables | Actual Meas. | Act. Crpt. Meas. | Est. Ukf Meas. | Est. Sr-ukf Meas. |
|--------------------------|--------------|------------------|----------------|-------------------|
| $e_{dq}$                 | -0.1584      | -0.1585          | -0.3784        | -0.1583           |
| $e_{ddq}$                | 0.2243       | 0.2245           | 0.0042         | 0.2242            |
| $e_{dd}$                 | -0.0152      | -0.0153          | -0.2352        | -0.0151           |
| $e_{ddd}$                | -0.0156      | -0.0161          | -0.2356        | -0.0155           |
| $\delta$                 | 4.0935       | 4.369            | 3.8735         | 3.7168            |
| $\omega$                 | 0.0048       | 0.0118           | -0.2152        | 0.0036            |

Table 3 quantify the estimation accuracy using error deviations (Root Mean Square Error). The SR UKF shows significantly smaller error deviations across all internal states and parameters. For example, the error deviation for  $e''_q$ , (1.768e-5) using SR UKF is, compared to 0.0389 for UKF, representing a substantial reduction in estimation error. Similar improvements are seen for both q -axis and d-axis parameters, with SR UKF achieving deviations as low as for, compared to the much larger deviations of UKF.

Table 3 The error deviation of the internal state variables

| Internal State Variables | Error dev. Ukf | Error dev. SrUkf |
|--------------------------|----------------|------------------|
| $e'_{q}$                 | 0.0389         | 1.768e-5         |
| $e''_{q}$                | 0.0389         | 1.768e-5         |
| $e'_{d}$                 | 0.0389         | 1.768e-5         |
| $e''_{d}$                | 0.0389         | 1.768e-5         |
| $\delta$                 | 0.0389         | 0.0666           |
| $\omega$                 | 0.0389         | 2.223e-4         |

Table 4 show the performance comparison between the Normal UKF and the SR UKF using the RMSE as the evaluation metric. The Normal UKF produced an RMSE of 0.5390, while the SR UKF achieved a

markedly lower RMSE of 0.1540. corresponding to a 71.4% reduction in estimation error. This substantial decrease indicates that the SR UKF significantly enhances the accuracy of the state estimation.

Table 4 The Performance index of the algorithms

| Performance | Normal Ukf | Improved Ukf |
|-------------|------------|--------------|
| RMSE        | 0.5390     | 0.1540       |

To better reflect real system conditions, white gaussian noise was added to the internal state variables with mean, covariance (0,0.001) and to the measured output with mean, covariance (0,0.1). Under these assumptions, the results of the SR-UKF algorithm for online state estimation of the sixth order nonlinear model of the synchronous generator subjected to a step on  $E_{fd}$  are presented in the following figures.

The black signals are the actual measured signal, which are corrupted with a white gaussian noise label as blue, the red signals are the estimated signals from the corrupted measured signals. The simulation time of the complete system is considered to be (5sec), since the point of interest are the transients and sub-transient's components the dynamic system to be tracked from noisy measurements.

Figures 1-3 show the actual measurement signal, corrupted measurement signal and estimated signal of transient voltages, sub-transient voltages, reactance, transient time constant and sub-transient time constant respectively. It is found that SR-UKF can estimate all parameters and state variables with good accuracy. Comparing the estimated values with the standard range values, it was observed that the estimated parameters fall within the range of Hydrogeneration units.

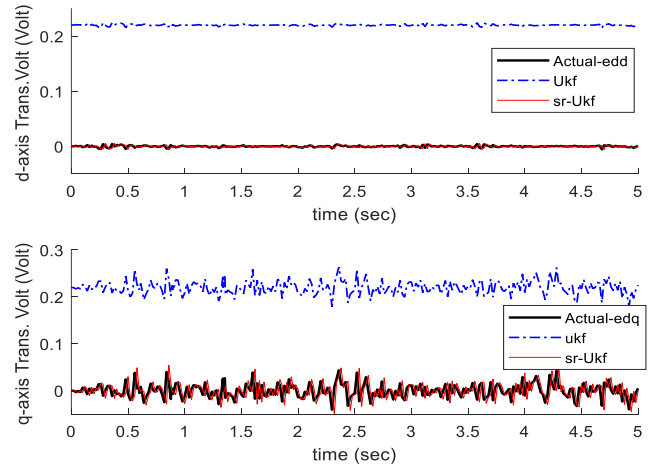


Figure 1 The Estimated Tran Voltage d-q axis of Electrical Model from Noisy Measurement

The figure 1 shows the results compares the estimation of transient voltages along the d-axis ( $e'_d$ ) and q-axis ( $e'_q$ ). In this case, a clear difference between the two filters is observed. The UKF estimates show a persistent bias (offset) from the true system values, indicating reduced accuracy in capturing these states. On the other hand, the SR-UKF closely matches the actual responses, with minimal estimation error and without noticeable bias. This highlights the improved accuracy of SR-UKF when estimating internal electrical states of the synchronous generator.

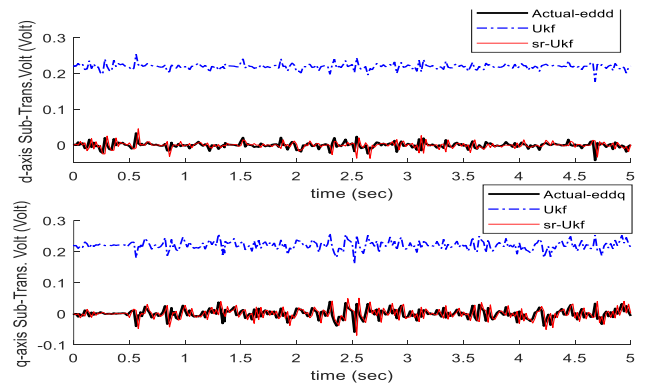


Figure 2 The Estimated Sub-Tran Voltage d-q axis of Electrical Model from Noisy Measurement

The figure 2 shows the results compares the estimation of sub-transient voltages along the d-axis ( $e''_d$ ) and q-axis ( $e''_q$ ). In this case, a clear difference between the two filters is observed. The UKF estimates show a

persistent bias (offset) from the true system values, indicating reduced accuracy in capturing these states. On the other hand, the SR-UKF closely matches the actual responses, with minimal estimation error and without noticeable bias. This highlights the improved accuracy of SR-UKF when estimating internal electrical states of the synchronous generator.

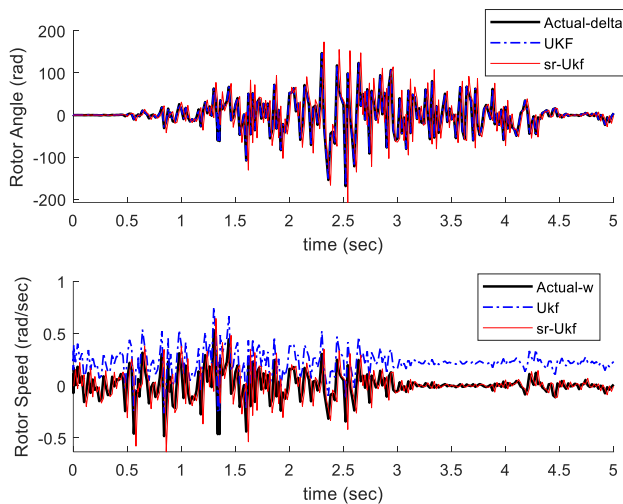


Figure 3 The Estimated State variable of Swing Equation Model from Noisy Measurement

Figure 3 shows the estimation of rotor angle and rotor speed deviation from noisy measurements. Both the UKF and SR-UKF were able to track the actual system states. However, the UKF estimates exhibited more fluctuations and sensitivity to measurement noise. In contrast, the SR-UKF produced smoother and more accurate estimates that were consistently closer to the actual system response. This demonstrates the superior numerical stability of SR-UKF in handling process and measurement noise.

## 5. Conclusion

The results obtained in this research highlight the potential of advanced filtering techniques in improving the accuracy and reliability of power system state estimation. While the Unscented Kalman Filter (UKF) proved effective in capturing the dynamics of a synchronous generator, its performance was occasionally limited by bias and noise sensitivity. In contrast, the Square Root Unscented Kalman Filter (SR-UKF) consistently provided more accurate, smoother, and noise-resilient state estimates. The

square-root covariance factorization enhanced numerical stability and prevented divergence, making the SR-UKF a more robust solution for nonlinear state estimation. It is therefore concluded that the SR-UKF is a more reliable tool for both state estimation and parameter identification of synchronous generator models. Its adoption in power system analysis and monitoring would significantly improve the quality of real-time decision-making, especially in environments characterized by measurement disturbances and uncertainty.

## References

- [1] J. A. Melkebeek, *Electrical Machines and Drives Fundamentals and Advanced Modelling*, Springer International Publishing AG, 2018.
- [2] J. Machowski, Z. Lubosny, J. W. Bialek, and J. R. Bumby, *Power system dynamics: stability and control*, John Wiley & Sons, 2020.
- [3] M. A. González-Cagigal, J. A. Rosendo-Macías and A. Gomez-Exposito, "Parameter Estimation of a fully regulated synchronous generators using Unscented kalman filter," *Elsevier Electric power systems Research*, p. 8, 2019.
- [4] S. Jiang, J. Shi, and S. Moura, "A New Framework for Nonlinear Kalman Filters," *arXiv preprint arXiv:2407.05717*, 2024.
- [5] H. G. Aghamolki, Z. Miao, L. Fan, W. Jiang, and D. Manjure, "Identification of synchronous generator model with frequency control using unscented Kalman filter," *Elsevier Electric power systems Research*, p. 10, 2015.
- [6] M. Ariff, M. B. Pal, and A. K. Singh, "Estimating dynamic model parameters for adaptive protection and control in power system," *IEEE Transactions on Power Systems*, vol. 30(2), pp. 826-839, 2014.
- [7] M. Chaabane, I. Baklouti, M. Mansouri, N. Jaoua, H. Nounou, M. Nounou, A. B. Hamida, and M. F. Destain, "Nonlinear state and parameter estimation using iterated sigma point kalman filter: Comparative studies," *Nonlinear Systems-Design, Analysis, Estimation and Control*, 2016.
- [8] P. Kundur, *Power System Stability and Control*, McGraw-Hill, Inc, 1994.
- [9] P. T. E. Cari, and L. F. C. Alberto, "Parameter Estimation of Synchronous Generators from Different Types of Disturbances," *IEEE Transaction on Power System*, p. 7, 2011.
- [10] D. F. Milano, *Power System Modelling and Scripting*, Springer Verlag London Limited, 2010.